Sensors & Transducers, Vol. 245, Issue 6, October 2020, pp. 20-26

Sensors & Transducers
Published by IFSA Publishing, S. L., 2020
http://www.sensorsportal.com

Design Approach for an Off-diagonal Giant Magneto Impedance Sensor Based on Field Programmable Gate Array

[1, *] Papa Silly TRAORE, [2] Aktham ASFOUR and [2] Jean Paul YONNET
[1] Ecole Supérieure Polytechnique (ESP), Université Cheikh Anta Diop (UCAD), Dakar, Sénégal
[2] Univ. Grenoble Alpes, CNRS, Grenoble INP, G2ELab, 38000 Grenoble, France
[1] Tel : +(221)773999941
[*] E-mail: papasilly.traore@esp.sn

Received: 25 September 2020 /Accepted: 23 October 2020 /Published: 30 October 2020

Abstract: This paper presents of a design approach for a high sensitivity digital off diagonal Giant Magneto Impedance (GMI) sensor based FPGA integrated circuits. The proposed design includes a Direct Digital Synthetizer (DDS) and a Digital Down Converter (DDC) fully implemented in the FPGA and associated with the off-diagonal configuration. This magnetic configuration has the potential to improve the sensitivity by increasing the number of turns of the pick-up coil and to realize a sensor without using a difference amplifier that could be source of additional noise. An equivalent magnetic white noise level of 1.1 pT/√Hz is measured. These results are achieved using a CoFeSiB micro wire of 2.5 cm length and 400 turns of coil wound around it. Results show that this white noise floor is mainly attributed to the Analog to Digital Converter (ADC).

Keywords: Giant Magneto Impedance (GMI), Off-diagonal configuration, Digital electronic conditioning.

1. Introduction

Since its discovery in 1991, the Giant Magneto Impedance effect (GMI) continues to attract the interest of the scientific community for the development of high sensitivity magnetic measurement devices [1]. The GMI effect is defined as a significant change of the ac impedance of some soft ferromagnetic conductor supplied by a high frequency (HF) excitation current, i_{ac}, and submitted to an external magnetic field. GMI sensors offer several advantages compared to conventional sensors. Some of the decisive advantage is the high sensitivity, the potential for miniaturization and the low energy consumption [2]. When a GMI element (generally an amorphous ferromagnetic material) is submitted to an external magnetic field to be measured, the voltage across the GMI element is amplitude modulated by the measured field. A demodulator is generally used to have the information of the measured field. A typical characteristic of the GMI effect is shown in Fig. 1.

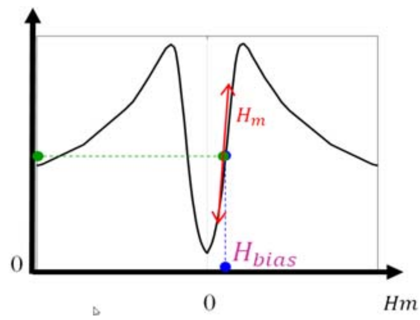

Fig. 1. Typical characteristic of GMI effect.

http://www.sensorsportal.com/HTML/DIGEST/P_3168.htm

The GMI characteristic is strongly nonlinear. To realize a sensor, it is generally magnetically biased in the region having the maximum of sensitivity. This field biasing creates an offset corresponding to the impedance value at the bias point. This offset is often suppressed using a difference amplifier. A typical configuration of a GMI sensor require the GMI element and its associated electronic conditioning which is mainly made of a HF frequency oscillator for providing the i_{ac} current, the demodulator (generally a peak detector) associated to an offset cancelling devices as seen in Fig. 2.

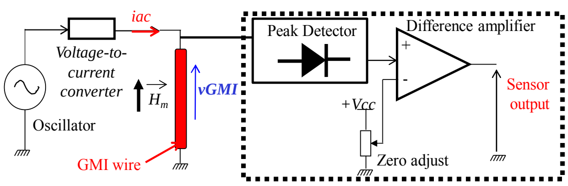

Fig. 2. Typical configuration of a GMI sensor.

One of the important features in GMI sensor limiting the detection performance is the equivalent magnetic noise level in T/√Hz which is a function of the electronic conditioning noise en_{sensor} in V/√Hz , the magnetic noise, S_{mag} in T/√Hz, and the sensitivity of the open loop sensor, S_c in V/T, as expressed in (1).

$$b_n = \sqrt{\frac{e^2_{n_{total}}}{S^2_c} + S^2_{mag}} \quad (1)$$

Usually, this noise spectral density or the equivalent magnetic noise level can be separate into a low-frequency excess (1/*f*) noise attributed to the fluctuations of the magnetization movement and a white noise region due to the electronic conditioning [3, 4]. Several studies show that, in a typical configuration of GMI sensor, the white noise equivalent magnetic noise level is attributed to the analog electronic conditioning noise and not by the intrinsic noise of the GMI element since all GMI sensors are associated to analog conditioning electronics [3].

In [5-7], we have introduced the digital concept in GMI sensor in order to reduce the electronic conditioning noise in the white noise region. Moreover, the sensitivity of the sensor has to be improved also so as to enhance the equivalent magnetic noise. The adopted solution to improve the sensitivity in GMI sensors is to use the sensing element in off-diagonal configuration. It consists of using a pick-up coil around the GMI sensing element [3]. The off diagonal configuration is explained by the Inverse Weidman effect [8, 9]. It is based on the appearance of a longitudinal magnetization in a ferromagnetic magnetic material which is circumferentially magnetized by the i_{ac} excitation current. One of the main advantages of this magnetic configuration is the potential for improving the sensitivity by increasing the number of turns of the pick-up coil.

This paper presents a design approach of GMI sensor based on digital concept and associated to the sensing element in off diagonal configuration. It is organized as follows. The hardware architecture of the digital GMI sensor is described in Section II. Section III presents the design approach from noise point of view and the prediction of the noise performance in the white noise region is presented. Results are given in Section IV. Finally, Section V gives a general conclusion.

2. Hardware Architecture of a Digital GMI Sensor

The hardware architecture of the proposed design is shown in Fig. 3. All the analog electronic conditioning is replaced by the digital concept. It is mainly made of a Direct Digital Synthetizer (DDS), the voltage-current converters, the sensing element in off-diagonal configuration and the detection stage (including a preamplifier, an Analog-to-digital converter (ADC) and a Digital Down Converter (DDC)).

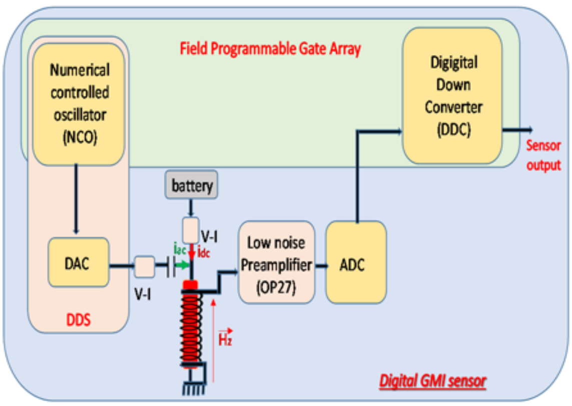

Fig. 3. Hardware architecture of the off-diagonal GMI sensor using a Direct Digital Synthesizer (DDS) and a Digital Down Converter (DDC) implemented using a Field Programmable Gate Array (FPGA).

The proposed sensor is based on a Field Programmable Gate Array (FPGA) [10, 11]. FPGA are configurable integrated circuits used to design digital functions. Their configuration is usually specified using hardware description languages such as VHDL or Verilog. Configurable Logic Block (CLB) (which is the basic element of an FPGA) are fundamental logical resources used to implement combinatory and sequential functions. They mainly consist of Look-up Table (LUT), multiplexers and D flip-flop. The CLB can be used to create complex logic functions but also as variable storage elements. This structure makes the FPGA architecture effective since any digital design uses these resources simultaneously. The novelty of this work, lies mainly in the fact that the DDS and DDC, required in the sensor implementation, are fully implemented on the FPGA.

2.1. The DDS

DDS is a technology that uses digital circuits to generate a programmable frequency output signal from a reference clock (125 MHz in our design) and a binary number (image of the desired frequency). The hardware architecture of the implemented DDS is shown in Fig. 4. The core of the DDS is the NCO, which integrates a phase-to-amplitude converter (usually a LUT) and a phase accumulator implemented to generate an appropriate phase argument. This phase argument is mapped to the address bus of the LUT which carries out the phase-to-amplitude conversion [10]. The DDS supplies the HF excitation current for the off-diagonal GMI sensing element. This DDS is mainly made of a Numerical Controlled Oscillator (NCO) implemented in the FPGA and associated to a Digital-to-Analog Converter (DAC). The DDS output is applied to a voltage-to-current converter (V-I) generally based resistor for supplying the i_{ac}, current for the GMI element.

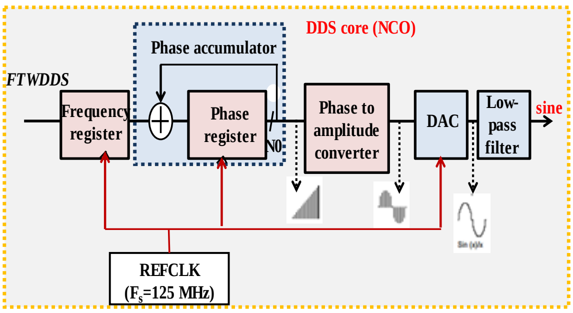

Fig. 4. Hardware architecture of the Direct Digital Synthetizer implemented in a Field Programmable Gate Array (FPGA).

2.2. The sensing Element

When the sensing element is subjected to the magnetic field, H_m, to be measured, a voltage, v_{coil}, is induced across the pick-up coil. This induced voltage results in fact from a cross magnetization process based on the appearance of an ac longitudinal magnetization in a ferromagnetic material (the GMI wire in this study) which is excited by a circumferential magnetic field created by the HF excitation current [12]. This longitudinal magnetization explains the appearance of the voltage across the pick-up coil. To observe this longitudinal component of magnetization, static magnetization must follow a helical path around the direction of the excitation current. Such magnetic structure can be obtained in GMI wire with circumferential anisotropy by using a dc current, I_{dc} which is superimposed to the i_{ac} excitation current. The dc field (creates by the dc current) combined with the axial field to be measured, H_m, (see Fig. 2), produces a helical magnetization which magnetizes the conductor along a helical path. That's why, in the current design, a static current, I_{dc}, is supplied to the GMI wire using a battery associated with a V-I converter generally based resistor. The use of this static current has also been shown to reduce magnetic noise [13].

2.3. The detection Stage

The voltage across the pick-up coil is optionally amplified by a low-noise preamplifier before being digitized by a high speed analog-to-digital converter (ADC) at a 125 MHz sampling frequency. At the output of the ADC, data are then transmitted to the Digital Down Converter implemented in FPGA for a digital quadrature lock-in detection that provides both the In-phase 'I' and the Quadrature 'Q' signals. Fig. 5 shows the block diagram of the Digital Down Converter. This DDC include NCO, digital mixing, rounding circuit, and a cascade of two low pass decimation filter: a Cascaded Integrator Comb decimation filter (CIC) and a Finite Impulse response filter (FIR).

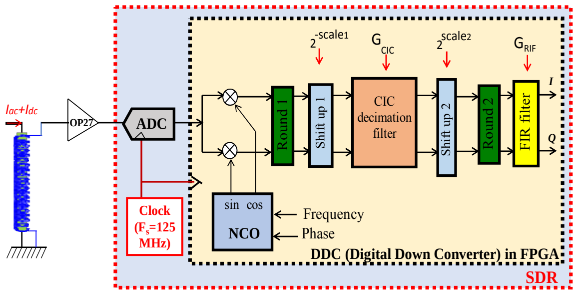

Fig. 5. Hardware architecture of the Digital Down Converter implemented in a Field Programmable Gate Array (FPGA).

The operating principle is as follows: Data at the ADC output is first digitally processed before being filtered by a cascade of the two low-pass digital filter: the CIC decimation filter (known as Hogenauer filters) [14] and the FIR filter. In our design, rounding circuits are necessary for real-time implementation since only a finite number of bits can be processed by the hardware. This DDC also includes Shift-up circuit that allow to set the digital gain. The intrinsic gain, G_{DDC}, of the DDC is given by:

$$G_{DDC} = 2^{-scale1} * G_{CIC} * 2^{scale2} * G_{FIR}, \quad (2)$$

where $scale_1$ and $scale_2$ are programmable digital coefficient in order to amplify or attenuate signal in the DDC; G_{CIC} and G_{FIR} are the intrinsic gain of the CIC filter and the FIR filter, respectively.

3. Noise Analysis

This section is related to the identification of each noise sources of the proposed design. The different noise sources involved in a digital GMI sensor are: the excitation system noise, the noise of the sensing element and its preamplifier, the ADC noise and the DDC noise.

3.1. The Excitation System Noise

The noise of the excitation system includes the DDS noise and the two voltage-current converters noise. Usually, the sinusoidal signal instability is characterized by the single-sideband noise spectral density expressed in decibels below the carrier per hertz (dBc/Hz) [15]. In a DDS, the white noise floor is mainly attributed to the DAC at its output [16]. For the used DDS, a white noise floor of about −149 dBc/Hz for a 125 MHz reference clock is obtained [17].

The second source of noise to consider in the excitation system is the well-known Johnson noise of both associated resistors.

In our design, the white noise floor of the excitation system (DDS noise floor and Johnson noise) is seen at the sensor output by the transfer function of the off-diagonal configuration [7]. Fig. 6 shows an example of characteristic obtained using the off-diagonal configuration. Since this magnetic configuration has the advantage of having an intrinsically zero response of the impedance at null field (i.e. odd function), choosing a bias field H_{bias}=0 A/m allow to roughly reduce the excitation system noise at the sensor output.

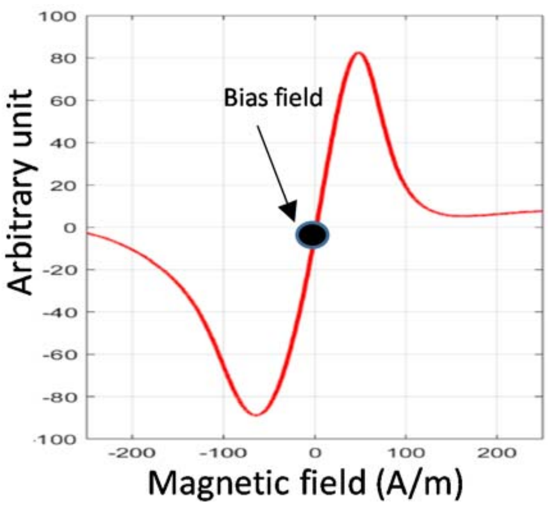

Fig. 6. Intrinsic response of the off diagonal configuration.

Moreover, this characteristic of the magnetic configuration is very suitable to realize a sensor without using an offset cancelling devices which can add noise.

3.2. The Sensing Element Noise and the Preamplifier

In the sensing element, two noise sources have to be considered: the magnetic noise linked to fluctuations of the magnetization movement of the GMI wire and the thermal noise linked to fluctuations of the active power of the GMI wire and the pick-up coil [3]. For the preamplifier which acts only as an impedance adapter between the sensitive element and the ADC, it must be chosen so that its equivalent input noise is much lower than that of the ADC [18]. In our implementation, the low noise OP27 preamplifier is used.

3.3. The ADC Noise

At the output of the preamplifier, the voltage is transmitted to the ADC which is one of the major elements of the digital concept. The ADC is characterized by: its input dynamic corresponding to the full scale, V_{FS}, and its resolution corresponding to its effective number of bits *ENOB*. Currently, the used converter is a 11-bit converter with a dynamic range of 2 V [19]. The quantum q corresponding to the Least Significant Bit (LSB) designates the smallest input change that allows obtaining a bit change at the output. It is given by:

$$q = \frac{V_{FS}}{2^{ENOB}} \tag{3}$$

During the analog-to-digital conversion a difference at the origin of the quantization noise appears between the digitized voltage and the actual analog voltage. Assuming that this noise is uncorrelated to the input signal and it is uniformly distributed between the quantization levels, the RMS value of the ADC noise, V_{noise}, is given by [20]:

$$V_{noise} = \frac{q}{\sqrt{12}} \tag{4}$$

In practice, this noise is uniformly distributed in the Nyquist bandwidth [0; F_s / 2]. Thus, the voltage noise spectral density (in V/√Hz) of the ADC, en_{ADC}, can be evaluated by:

$$e_{n_{ADC}} = \frac{V_{Fs}}{2^{ENOB}\sqrt{6F_s}} \tag{5}$$

3.4. The DDC Noise

Data at the ADC output is then transmitted to the DDC for digital synchronous demodulation. In the digital concept, the considered noise source is the noise due to the suppression of certain bits also called computation noise or rounding noise essential during digital processing on FPGA. In fact, consider an input data y_{in} (at the input of the Round circuit) and an output data y_{out} (at the output of the Round circuit) represented in 2's complement as expressed in Eq. (6), Eq. (7) and illustrated in Fig. 7.

$$y_{in} = -2^{-m} S + \sum_{i=0}^{m-1} Z_i 2^i , \qquad (6)$$

$$y_{in} = -2^{-m} S + \sum_{i=p}^{m-1} Z_i 2^i , \qquad (7)$$

where p denotes the number of suppressed bits due to rounding operation, m represents the number of bits at the input of the Round circuit, S is the sign bit and z_i denote the coefficients associated with the powers of 2^i. These coefficients can take two values 0 or 1.

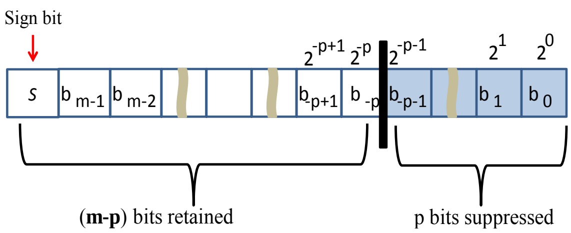

Fig. 7. Representation of data during bit suppression.

The rounding noise results from the difference between the two variables y_{in} and y_{out} due to the suppression of least significant bit (LSB) since only a finite number of bit can be processed by the hardware. So that noise from digital processing in the FPGA implementation does not degrade the overall noise performance of the sensor, the size of the computing accumulators in the DDC at the output of each digital circuit must be chosen so that the LSB of each circuit is much lower than that of the ADC [19]. As a result, the voltage noise spectral density and hence the equivalent magnetic white noise level could be limited by the ADC. Fig. 8 shows a block diagram of the different noise sources of the sensor [21].

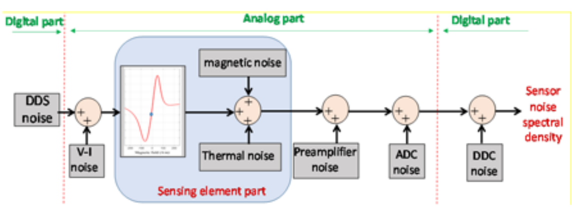

Fig. 8. Bloc diagram of different noise sources involved in a digital GMI sensor.

4. Results

Noise measurement have been conducted in order to validate the proposed design approach. The sensitive element was a CoFeSiB wire (25 mm long and 100 µm diameter) with a 400-turn pick-up coil. The excitation current, i_{ac}, was 1 MHz of frequency and 7 mA of amplitude. To be sure of the proper functioning of the sensor, a reference signal (70 nT_{rms} peak amplitude, 30 Hz frequency) was applied to the sensor. A DC current of 4 mA was also used. The digital gain of the DDC was set to around 40. With this setting and using an ADC sampled at 125 MHz with an effective number of bit of 11, a voltage noise spectral density of approximately 1 µV/$\sqrt{\text{Hz}}$ is measured in the white noise region. Fig. 9 shows the measured noise spectral density of the sensor. With respect to the proposed design approach, we can observe that the white noise floor of the sensor is mainly due to the ADC which has an equivalent noise contribution of 0.98 µV/$\sqrt{\text{Hz}}$ according to Eq. (5).

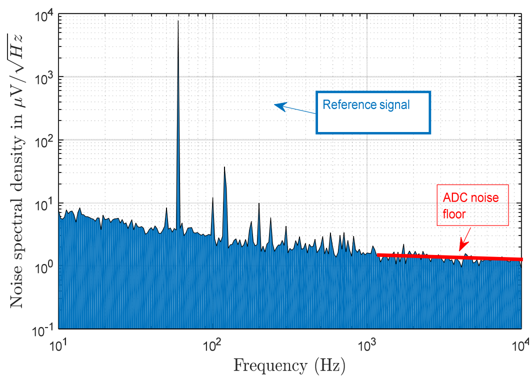

Fig. 9. Voltage Noise spectral density of the digital sensor; The excitation parameters are Iac = 7 mA, Idc = 4 mA. The digital gain of the DDC was about 40. Bandwidth at -3 dB = 41 kHz.

The equivalent magnetic noise is then measured. It is obtained by the ratio between the measured voltage noise spectral density and the measured sensitivity of the sensor. In this configuration, a sensitivity of about 0.9 MV/T was measured. This yields to a measured equivalent magnetic noise level of 1.1 pT/$\sqrt{\text{Hz}}$ in the white noise region and 10 pT/$\sqrt{\text{Hz}}$ at 10 Hz. This equivalent magnetic (E_{MN}) noise can be estimated in the white noise region as:

$$E_{MN} = \frac{e_{n_{ADC}}}{S_\Omega I_{ac}} = \frac{V_{Fs}}{S_\Omega I_{ac} 2^{ENOB} \sqrt{6F_s}} \qquad (8)$$

where S_Ω denotes the intrinsic sensitivity of the GMI element in off-diagonal configuration (expressed in Ω/T) and I_{ac} is the amplitude of the excitation current from the DDS.

This noise level is roughly comparable with one reported in the state of the art. For example, [22, 8] presents devices integrating a complete implementation of a magnetometer. The obtained performances are around 17 pT/√Hz at 1 Hz with a sample based CoFeSiBCr in off-diagonal configuration (11 cm length and 490 turns).

Table 1. White noise performances for the one reported in the state of the art.

REF	Configuration	Sensing element	Excitation	Detection	White noise equivalent magnetic noise level
[8]	Orthogonal fluxgate in fundamental mode	4.5 mm length 480 turns	I_{ac}=12 mArms I_{dc}=24 mA F=100 kHz	AD630	2.5 pT/√Hz
[24]	Off diagonal	Ribbon with creep-induced anisotropy (11 cm long, 1.2 mm width and 17 mm thick)	I_{ac}=10 mArms I_{dc}=20 mA F=300 kHz	SR840	8 pT/√Hz
[25]	Off diagonal	Ribbon of 11 cm long; 290 turns is wound on fiberglass tube of 9 mm diameter, in which the ribbon is inserted	I_{ac}=50 mArms I_{dc}=10 mA F=360 kHz I_{ac}=30 mArms I_{dc}=10 mA F=360 kHz	SR844 SR844	4 pT/√Hz 0.7 pT/√Hz Obtained with suppressed carrier
[3]	Off diagonal	Microwire COFESIB (2.5 cm × 1 mm × 100 µm of diameter) 1000 turns	Iac=13 mArms Idc=6 mA *F*=1 MHz	Peak detector	0.9 pT/√Hz Feedback on the pick-up coil 1.5 pT/√Hz Feedback on an external solenoid
This work	Off diagonal	Microwire COFESIB (2.5 cm × 100 µm of diameter) 400 turns	Iac=7 mArms Idc=4 mA *F*=1 MHz	Digital Down Converter	1.1 pT/√Hz

In view of this good performance, special attention must be paid to the length of the sensitive element because the intrinsic sensitivity of the GMI device is inversely proportional to the volume of the sample. For the same diameter, an increase in length results in a reduction in the equivalent magnetic noise level. Noise performances of 30 pT/Hz and 4 pT/√Hz respectively at 1 Hz and in a white noise region are obtained in [23]. It emerges from this work that 1/f noise is related to the magnetic noise of the sensitive element and the white noise floor is dominated by the conditioning electronics. Performances were subsequently improved by a carrier suppression to finally reach a level of 0.7 pT/√Hz in the white noise region. [24], more recently, obtained performances of 30 pT/√Hz and 15 pT/√Hz respectively at 1 Hz and in white noise zone with a demodulator based on a TAD (Time Analog to Digital). The performance obtained in a white noise zone is not necessarily competitive with regard to the current state of the art. [3] shows a complete approach for the realization of an optimized magnetometer. The sensing element was a microwire of 2.5 cm lentgh. Noise performances of 35 pT/√Hz and 0.9 pT/√Hz at 1 Hz and in white noise region respectively. This results are obtained with a feedback on an external solenoid. Then for a feedback on the pick-up coil, they present performances of 35 pT/√Hz and 1.5 pT/√Hz at 1 Hz and in white noise region respectively. This performance is among the best in the current state of the art of GMI sensors. In summary, the best current performance of GMI sensors is around pT/√Hz in a white noise region for a typical off-diagonal GMI sensor with a reasonable size.

From these noise levels perspectives, the integration of the digital concept in GMI sensors opens up a wide range of applications. These performances can be improved by decreasing the noise spectral density of the ADC since it limits the white noise performance. According to Eq. (5), this noise spectral density can be reduced by using a converter with a higher resolution (i.e. a larger effective number of bits) or a converter sampled at a higher sampling rate. However, this brings us to a technological limitation to overcome since, generally, the increase of an ADC resolution results to a decrease of the sampling rate.

For a typical off-diagonal sensor of reasonable size (approximately, a few centimeters length and a few hundred turns for the pick-up coil), another limitation of the current digital design is related to the input dynamic range of the used ADC. The full scale dynamic range of 2 V establishes a maximum limit on the amplitude that could be applied to the ADC input. This avoids the use of higher *ac* excitation current and higher preamplifier gain to improve sensitivity before sampling. This results to a maximum sensitivity at the input of this available converter. The use of an ADC with a higher dynamic is therefore necessary to increase the sensitivity and thus reduce the equivalent magnetic noise of the sensor.

5. Conclusion

The design approach of a digital off-diagonal GMI sensor based Field Programmable Gate Array (FPGA) is presented. The proposed architecture combines the off-diagonal configuration and the digital concept so as to realize a high sensitivity sensor. This magnetic configuration has the potential on the one hand to reduce the noise from the excitation system and on the other hand to realize a sensor without using an offset cancelling devices. Performances of 1.1 pT/√Hz are obtained in the white noise region. The obtained results show that the white noise floor is mainly attributed to the ADC. Finally, further methods to improve the white noise performance were proposed.

References

[1]. E. P. Harrison, G. L. Turney, H. Rowe, Electrical properties of wires of high permeability, *Nature*, Vol. 135, Issue 3423, 1935, pp. 961.

[2]. Magnetic sensors and magnetometers, Ed. Pavel Ripka, *Artech House,* 2001.

[3]. B. Dufay, S. Saez, C. P. Dolabdjian, A. Yelon, D. Ménard, Characterization of an optimized Off-diagonal GMI-based Magnetometer, *IEEE Sensor Journal*, Vol. 13, Issue 1, January 2013, pp. 379-388.

[4]. D. Ménard, D. Seddaoui, L. G. C. Melo, A. Yelon, B. Dufay, S. Saez, C. Dolabdjian, Perspectives in Giant Magnetoimpedance Magnetometry, *Sensors Letters*, Vol. 7, Issue 3, 2009, pp. 429-432.

[5]. P. S. Traore, A. Asfour, J.-P. Yonnet, Implementation of the Digital-Down-Conversion (DDC) and software for the optimization of the Giant Magneto-Impedance (GMI) sensors, *IEEE SENSORS*, 1-4 November 2015.

[6]. P. S. Traore, A. Asfour, J.-P. Yonnet, Noise investigation of a GMI sensor utilizing a digital synchronous detector, in *Proceedings of the 11th European Magnetic Sensors and Actuators Conference (EMSA'16)*, Turin, Italy, 2016.

[7]. P. S. Traore, A. Asfour, J.-P. Yonnet, Noise Performance of SDR-Based Off-diagonal GMI Sensors, *IEEE Sensors Journal*, Vol. 17, Issue 19, April 2017.

[8]. L. Kraus, M. Malatek, M. Dvorak, Magnetic field sensor based on asymmetric inverse Wiedemann effect, *Sensors and Actuators A: Physical*, Vol. 142, Issue 2, 2008, pp. 468-473.

[9]. A. S. Antonov, I. T. Iakubov, A. N. Lagarkov, Longitudinal-transverse linear transformation of the HF-current in soft magnetic materials with induced anisotropy, *IEEE Transactions on Magnetics*, Vol. 33, Issue 5, 1997, pp. 3367-3369.

[10]. P. S. Traoré, A. Asfour, J.-P. Yonnet, C. Boudinet, Introduction of real-time digital processing techniques for the high-sensitivity GMI sensors, *International Journal of Applied Electromagnetics and Mechanics*, Vol. 59, Issue 2, 2019, pp. 455-463.

[11]. S. Traoré, A. Asfour, J.-P. Yonnet, C. Boudinet, Digital Electronic Conditioning Approach for the High Sensitivity Off-diagonal GMI Sensors, *Sensors and Actuators A: Physical*, Vol. 271, March 2018, pp. 290-302.

[12]. S. Sandacci, D. Makhnovskiy, L. Panina, K. Mohri, Y. Honkura, Off-diagonal impedance in amorphous wires and its application to linear magnetic sensors, *IEEE Transactions on Magnetics*, Vol. 40, Issue 6, Nov. 2004, pp. 3505–3511.

[13]. E. Paperno, Suppression of magnetic noise in the fundamental-mode orthogonal fluxgate, *Sensors and Actuators A: Physical*, Vol. 116, Issue 3, October 2004, pp. 405–409.

[14]. Eugene B. Hogenauer, An economical class of digital filters for decimation and interpolations, IEEE Transactions on Acoustics, Speech and Signal Processing, Vol. 29, Issue 2, 1981, pp. 155-162.

[15]. L. Ding, Étude et amélioration des performances en bruit de capteurs à MagnétoImpédance Géante: Application à la magnétométrie à très haute sensibilité, *Thèse de Doctorat en Électronique et Microélectronique*, Université de Caen, 2008.

[16]. Jouko Vankka, Direct Digital Synthesizers: Theory, Design and Applications, *Springer US,* 2000.

[17]. DAC1401D125, Dual 14-bit DAC, up to 125 Msps Data sheet, NXP Semiconductors, January 2012.

[18]. P. S. Traore, A. Asfour, J.-P. Yonnet, Implementation rules for optimized noise performance in digital GMI sensor, *IET Journal* (submitted).

[19]. LTC2145, Low power dual ADCs Data sheet, Linear Technology, McCarthy, USA, 2011.

[20]. B. Widrow, A Study of Rough Amplitude Quantization by Means of Nyquist Sampling Theory, *IRE Transactions on Circuit Theory*, Vol. 3, Issue 4, 1956, pp. 266-276.

[21]. P. S. Traore, A. Asfour, P. A. Fam, J.-P. Yonnet, High Sensitivity digital GMI sensor based FPGA, in *Proceedings of the 6th International Conference on Sensors and Electronic Instrumentation Advances (SEIA' 2020)*, 23-25 September Porto, Portugal, 2020, pp. 65-69.

[22]. M. Malátek, L. Kraus, Off-diagonal GMI sensor with stress-annealed amorphous ribbon, *Sensors and Actuators A: Physical*, Vol. 164, Issue 1-2, 2010, pp. 41-45.

[23]. M. Malatek, B. Dufay, S. Saez, C. Dolabdjian, Improvement of the off-diagonal magnetoimpedance sensor white noise, *Sensors and Actuators A: Physical*, Vol. 204, December 2013, pp. 20–24.

[24]. Shingo Tajima, Peng Wu, Yukihiro Okuda, Takatomo Watanabe, Tsuyoshi Uchiyama, Magneto-Impedance Sensor Based on Time Analog to Digital Converter (TAD) for Circuit Integration, *IEEE Transactions on Magnetics*, Vol. 51, Issue 11, Nov. 2015.

___